A panorama of phase transition signals and influence of collision-induced correlations

R. Bougault

A panorama of phase transition signals and influence of collision-induced correlations

R. Bougault for the INDRA and ALADIN collaborations

LPC Caen (IN2P3-CNRS/ENSICAEN et Université), F-14050 Caen Cedex , France

Abstract

The presented results will show the richness of nuclear heavy-ion physics where data are accumulated as a succession of independent events. The different reaction mechanisms can provide for 39 A.MeV Ta+Au, 40 and 80 A.MeV Au+Au peripheral collisions a set of data almost free of entrance channel effects as well as a set of events where collision-induced correlations can be evidenced. The event selection method will be presented and it will be shown how the entrance channel dynamical effects affect determination of heat capacity through partial energy fluctuation measurements.

1. Introduction

It is difficult to give a general and precise definition of a pure phase and the concept in itself finds its relevance if there exists different phases for a system. The question of phases of nuclear matter is therefore linked with the observation of a phase transition.

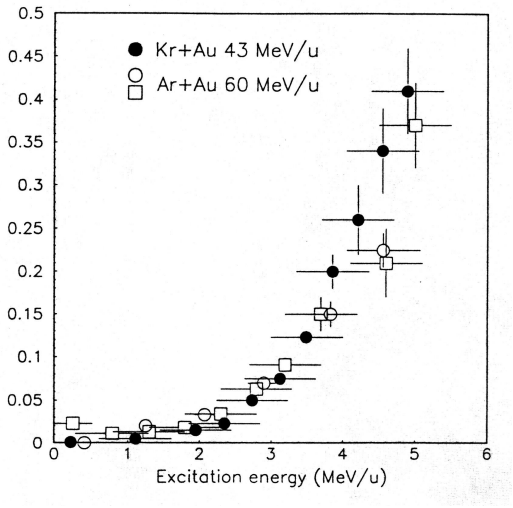

Figure 1: *Evolution of the 3-fragment over 2-fragment emission ratio as a function of the excitation energy [1].*

Experimentally (fig. 1) it has been evidenced, at around 3 A.MeV of excitation energy, a rapid increase of multifragment emission from excited nuclear systems formed in central collisions. This situation can be considered as a drastic change relative to the low excitation energy regime where only light particle evaporation process occurs. Since at high excitation energy vaporization events have been measured [2], it is then tempting to proceed through a liquid-gas description of nuclear matter and to consider the multifragment emission as a sign of a phase change.

2. Equilibrium

Experimentally the excited nuclear systems are prepared through collisions between projectiles and targets and the study of the equation of state is generally conducted through relevant variables as temperature, density,... related to an equilibrium situation for a given excitation energy. In these collision experiments, "data are accumulated as a succession of independent events. Thus (...) most nuclear physics experiments provide us with an ensemble of events. Considering that each event can be associated with a particular microscopic configuration of the system under study one might therefore consider the ergodic hypothesis to be unnecessary because experiment directly accesses an ensemble of microstates" [3]. It is indeed the dynamics of projectile and target collisions which provides us with such ensembles of events. The semantics of equilibrium is therefore related to a question of phase space filling and opens new perspectives [4] if one admits that the ergodic hypothesis is not necessary to our studies. We then speak of pseudo-equilibrium as the framework of statistical studies of ensembles of events produced by projectile and target colli-

sions.

3. Breaking points

In general the characterization of a phase transition is revealed by breaking points on curves of relevant variables which describe the system's thermodynamical states.

For infinite systems the quest of breaking points is independant of the ensemble since ensembles are equivalent. As an example for a constant pressure thermodynamical path at equilibrium, to a plateau in the caloric curve (temperature, energy) of a first order phase transition for a microcanonical ensemble does correspond a step on the (energy, temperature) plot for the corresponding canonical ensemble. Both curves are equivalent (fig. 2,3) : the expected signal is the same whatever the chosen ensemble.

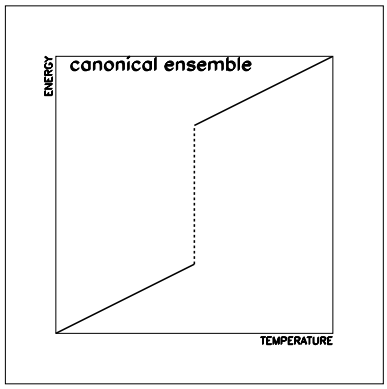

Figure 2: *canonical ensemble caloric curve*

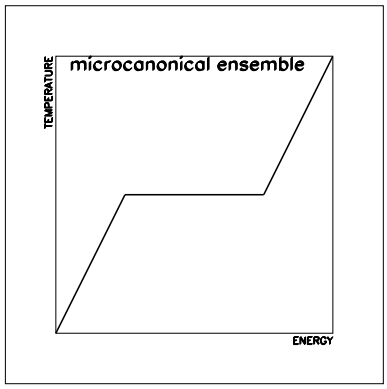

Figure 3: *microcanonical ensemble caloric curve*

For finite systems the situation is different [4]. There is a non-equivalence of the ensembles relative to a transition signal. Coming back to the example of a first order phase transition at constant pressure at equilibrium, the caloric curve will present a backbending in the microcanonical case and a change of slope without backbending for the canonical ensemble. More, the liquid gas phase transition for equilibrated finite systems is evidenced by a bimodal distribution of the order parameter in a canonical ensemble while this order parameter will present large fluctuations in the microcanonical case without necessarily being bimodal.

For a liquid gas phase transition, the particle density is the natural order parameter and therefore all experimentally accessible variables related to it are relevant variables which can be used to sign the transition. The size of the biggest cluster (A_{big}) is indeed a good choice because of its direct relationship with the particle density. Indeed isobar 6x6x6 lattice gas calculations [5] indicate a A_{big} bimodal distribution at the transition temperature (canonical case) while at the transition energy (microcanonical case) large fluctuations of the A_{big} distribution are produced (fig. 4). The ensembles are not equivalents, the canonical bimodality corresponds to the microcanonical large fluctuations.

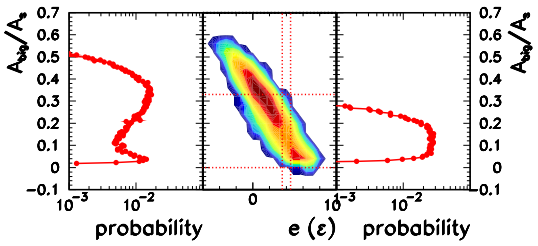

Figure 4: *Size of the biggest fragment normalized to the size of the system and its relationship with total energy in the canonical isobar lattice gas model at the transition temperature (centre and left). Size of the biggest fragment normalized to the size of the system in the microcanonical isobar lattice gas model at the transition energy (right).*

In the transition signal quest for finite systems it is therefore important to define the proper relevant variables according to the type of studied ensemble if one wants to extract a definite answer. The comparisons between differents data has to be performed with the same sorting variable and the choice of the relevant variables to

evidence a phase transition, i.e breaking points, is closely linked to the type of prepared ensemble.

4. Experimental signal situation

An experimental evidence of a phase transition has been claimed from the event by event study of partial energy fluctuations in Au Quasi-Projectiles formed in Au+Au collisions at 35 A.MeV (MULTICS-Miniball) [6] and in one source central events formed in Xe+Sn collisions at 32-50 A.MeV (INDRA) [7] [8]. For

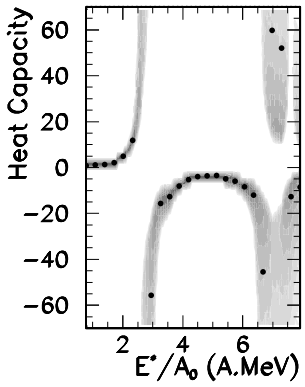

Figure 5: *Heat capacity (C) versus excitation energy (E^*/A_0) for Au-nucleus formed in peripheral Au+Au 35A.MeV [6]. From low to high E^*/A_0 : liquid phase (C>0), coexistence region (C<0) and gas phase (C>0).*

both sets of data, equilibrated events are selected and the excited source configuration is reconstructed through a calorimetrical analysis of its de-excitation products. For both types of selected events, the heat capacity is deduced from the partial energy fluctuations and shows a negative branch providing a signal expected for a first order liquid gas phase transition. For central INDRA events, signals of spinodal decomposition are also claimed [9] and their relationship with negative heat capacities is obvious [10]. For fig. 5, the set of events presents all the statistical characteristics of an ensemble of deexcitation schemes of an excited Au-nucleus and the equilibrium and pure thermal hypothesis has been tested through comparison with statistical models.

In this case, the data sorting has been done using E* bins since the expected signal only shows up in microcanonical ensembles where the phase transition is signaled by large fluctuations. A data sorting according to multiplicity or light particle transverse energy bins would have been a bad starting point to look for large fluctuations.

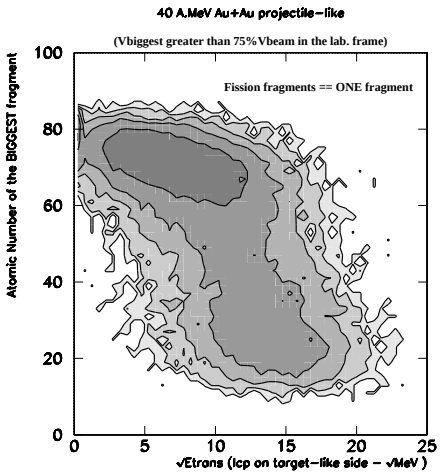

Figure 6: *Size of the projectile-like biggest fragment versus the square root of the light charged particle transverse energy detected on the target-like side for Au+Au 40 A.MeV.*

A different sorting, for the same events, is given by a pseudo-canonical ensemble of deexcitation schemes of an excited projectile-like. This can be done using the thermal characteristics of the coincident target-like nucleus. More precisely, the square root of the light charged particle transverse energy detected on the target-like side ($\sqrt{E_{trans}}$) can be seen as a thermometer and utilized as the sorting variable [11]. In this case the target-like nucleus is assumed to play the role of an approximate heat bath for the projectile-like. Fig. 6 presents the correlation between the size of the biggest projectile-like fragment (Z_{big}) and $\sqrt{E_{trans}}$ for the reaction 40 A.MeV Au+Au revealed by INDRA operating at the GSI facility. For the biggest projectile-like fragment it has been assumed that fission was acting as a secondary de-excitation process of a fragment whose atomic number is the sum of the two fissioning partners. We see a bimodal Z_{big} distribution for $\sqrt{E_{trans}}$ around 12 $\sqrt{MeV}$. We refer to [11] for experimental details about fig. 6. The purpose here is to show that it is possible to understand at the same time fig. 5 and fig. 6 in the context of a

phase transition : the first signal refers to a microcanonical sorting, the second to a canonical sorting, both signals are candidates to evidence the same phase transition.

5. An experimental ambiguity or contradiction

Fig. 5 refers to Au+Au 35 A.MeV (MULTICS-Miniball) reactions while fig. 6 to Au+Au 40 A.MeV (INDRA) reactions. Both retained projectile-like ensembles were selected in the same way and are supposed to be equivalent, i.e. independent of the detection apparatus. One expects therefore to find fig. 5 signal for the INDRA projectile-like data, when properly sorted according to excitation energy.

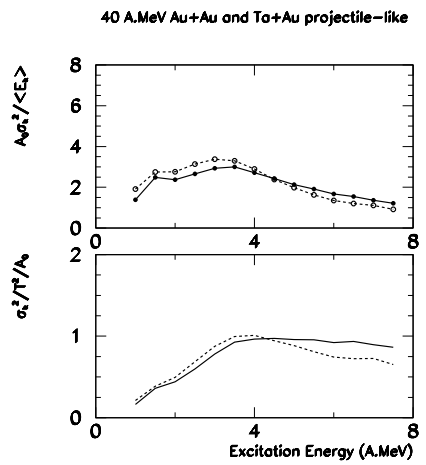

Figure 7: *Projectile-like partial energy fluctuations versus excitation energy for Au+Au 40 A.MeV (dashed line) and Ta+Au 39.6 A.MeV (full line) INDRA data. Top : partial energy fluctuation (σ_k) normalized to the mean partial energy ($< E_k >$), bottom : σ_k normalized to the projectile-like temperature. The Partial energy fluctuations have been scaled with the size of the projectile-like source ($A_0 \pm 10\%$).*

For the same selection as for MULTICS-Miniball data, the Au+Au 40 A.MeV and Ta+Au 39.6 A.MeV INDRA data have been analyzed. Partial energy fluctuations have been evaluated through a schematic freeze-out reconstruction hypothesis (hot fragment hypothesis) [6]. Both the excitation energy and the temperature of the projectile-like have been estimated using the same prescriptions as for MULTICS-Miniball data. The result, displayed in fig. 7, is quite surprising since partial energy fluctuations do not present any clear signal of growth around 4 A.MeV of excitation energy as it was expected from the comparison with MULTICS-Miniball projectile-like data (see fig. 11-left of [6]).

For INDRA projectile-like data selected as for MULTICS-Miniball data, the heat capacity does not show any negative values. The question is therefore to understand if this is an ambiguity or a contradiction.

6. Thermal equilibrium state versus external constraints

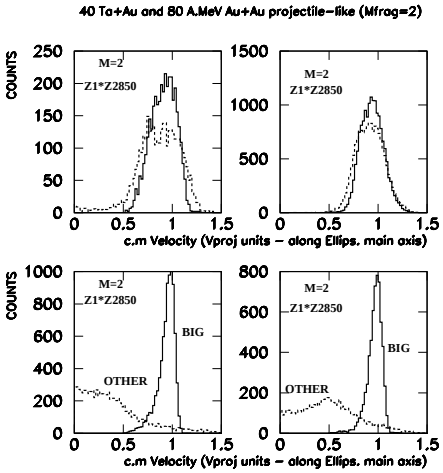

Figure 8: *Center of Mass velocity along the projectile-like direction of c.m forward detected fragments ($Z \geq 3$) in the case of 2-fragment events. Left : Ta+Au 39.6 A.MeV, right : Au+Au 80 A.MeV. Up : fission fragments ($Z_1 Z_2 \geq 850$), down : fragments for $Z_1 Z_2 < 850$. Full line is for the biggest fragment.*

As it was pointed out previously, it is indeed the dynamics of the collision which is responsible for the pseudo-equilibration state. However it is well established that dynamical effects play a role in multifragmentation at intermediate energies [12]. In the analysis presented above, the heat capacity is reconstructed assuming that the excitation energy of the projectile-like is of purely thermal origin. In other words, it is assumed that the set

of detected microscopic configurations represents all the possible deexcitation schemes of a thermal excited projectile-like fragment.

Fig. 8 represents the c.m forward topology of INDRA 2-fragment events in the projectile-like c.m direction (Ta+Au 39.6 A.MeV and Au+Au 80 A.MeV). While fission events present a statistical emission behaviour, this is not the case for events of high mass asymmetry. The majority of $Z_1 Z_2 < 850$ events are aligned along the beam direction [12] in velocity space. For 40 A.MeV incident energy, the lightest fragment is emitted with mid-rapidity velocity and for 80 A.MeV incident energy, it is emitted with a velocity intermediate between mid-rapidity and projectile velocity. For both bombarding energies, the biggest fragment is peaked at a too large velocity respect to a pure 2-body statistical process (i.e. 2 fragments from an excited projectile-like nucleus).

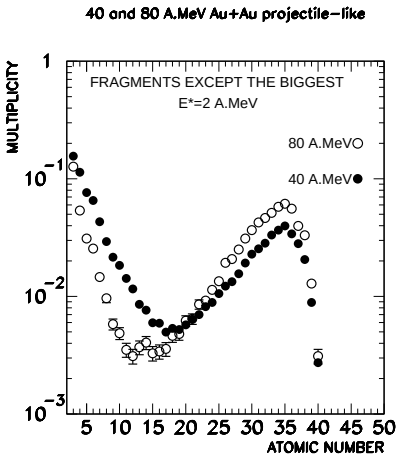

Figure 9: *Atomic number distributions in the c.m forward hemisphere for Au+Au 40 and 80 A.MeV (except the biggest fragment) for an excitation energy of 2±0.5 A.MeV. The excitation energy is calculated by calorimetry in the c.m forward hemisphere (as in [6]).*

It is clear here that the collision mechanisms interfer with the phase space filling, by adding external constraints. This has some consequences on the definition (i.e. selection) of the system (i.e. source) under study : the hypothesis of full equilibration of a source whose deexcitation schemes are represented by all the particle and fragments detected in the c.m forward direction is not valid for INDRA data. This can be simply and clearly evidenced by looking at the detected partitions. Assuming that the c.m forward emitted fragments represent a fully equilibrated source, then for the same system and same reconstructed excitation energy one should find the same partitions for different bombarding energies. Fig. 9 indicates large differences for Intermediate Mass Fragment production. The reconstructed fully equilibrated projectile-like is therefore largely hypothetical.

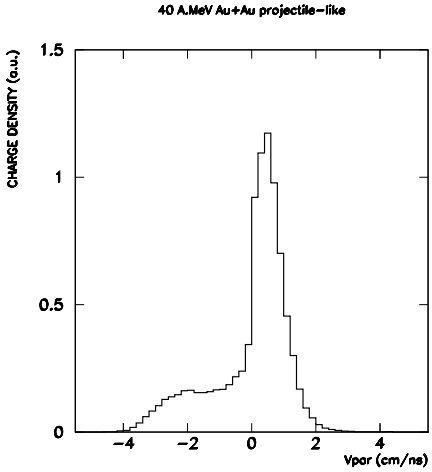

Figure 10: *INDRA Au+Au 40 A.MeV : fragment ($Z \geq 3$) charge density as a function of the parallel velocity in the hypothetical projectile-like source for E^*/A_0=3-4.5 A.MeV. The excitation energy is calculated by calorimetry in the c.m forward hemisphere (as in [6]) and the source velocity is given by c.m forward hemisphere emitted fragments.*

For MULTICS-Miniball data, it has been shown that the selected sample of events was not strongly influenced by collision-induced correlations. As an example, one can compare charge density distribution of MULTICS-Miniball fig. 1 of [13] with charge density for INDRA presented in fig. 10. For INDRA data, the collision-induced correlation effects cause the biggest fragment to be emitted preferentially on the forward part of the hypothetical source (projectile-like). For MULTICS-Miniball data this hierarchical effect is not strong. The selected sample is therefore not the same and it seems that the MULTICS-

Miniball sample represents a sub-sample of INDRA data.

7. Evidencing collision-induced correlations with INDRA data

In the previous section we have shown that for thermodynamics studies, one has to control the effects of collision-induced correlations which can affect the source selection and its pure thermal excitation hypothesis. For the moment, collision-induced correlations have been evidenced with one body observables (fig. 8, 9 and 10). We shall now use correlations within each event for a deeper study.

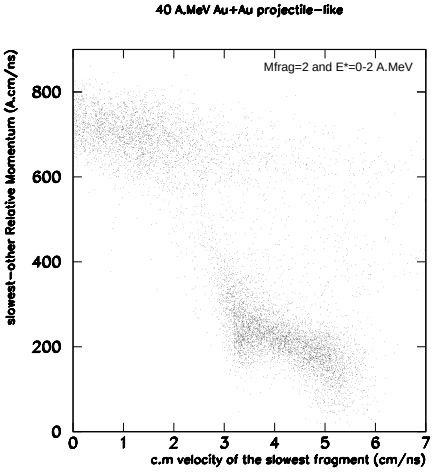

Figure 11: *Au+Au 40 A.MeV : fragment c.m relative momentum versus c.m velocity of the lightest fragment along the hypothetical projectile-like (Au) direction. This concerns reactions leading to 2 detected fragments in the forward c.m direction and Au excitation energy (calculated as in [6]) of 1±1 A.MeV. For compatibility with fig. 12 the label "slowest" has been used in the figure. It should be understood as the slowest fragment among fragments except the biggest, i.e. the lightest fragment for 2 detected fragments.*

Experimentally, if one wants to identify a fully equilibrated source, one needs to study its deexcitation schemes in the source frame. In the same way, if one wants to study collision-induced correlations, one needs to study the events in the frame where these dynamical effects occur (i.e. c.m), and use variables which magnify the effect. Both the aligment and hierarchical effects along the projectile direction are contained in the fragment c.m relative momentum (p_{rel}) in the case of 2-body forward detected fragments ($Z \geq 3$). The effect is magnified if one plots p_{rel} against the velocity of the slowest detected fragment as it is done in fig. 11. Fission fragments correspond to p_{rel} values around 200 A.cm/ns, while fragments emitted at mid-rapidity are situated in the upper left corner. It is clear also that two event families exist in the figure : mid-rapidity events seem to correspond to higher p_{rel} values rather than to a well localized velocity group. In the vernacular of heavy-ion physicists, the word "mid-rapidity" is often used to define many different processes from neck emission to participant source. For our purpose here, we just want to evidence that collision-induced correlations are related to high values of p_{rel} and correlated to a large domain of velocity values.

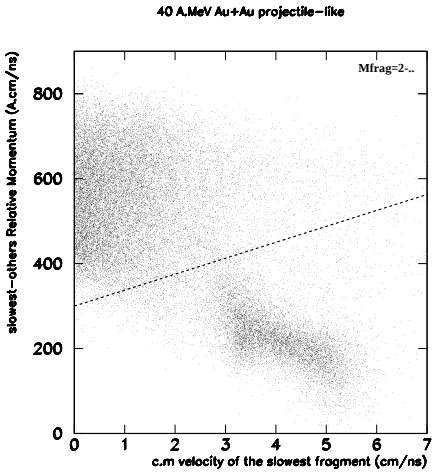

Figure 12: *Au+Au 40 A.MeV : same as fig. 11 for 2,3,... detected fragments in the forward c.m direction (no selection on excitation energy). The label "slowest" should be understood as the slowest fragment among fragments except the biggest.*

The p_{rel} velocity correlation of fig. 11 can be generalized to higher fragment multiplicities by grouping fragments in two sets. Since we have noticed from above the specific role of the biggest fragment and the c.m slow velocity component, the following classification has been adopted : on one side the slowest fragment among fragments

except the biggest, on the other side the rest including the biggest fragment. p_{rel} is now the c.m relative momentum between the two sets. The result is presented in fig. 12, we can see that the zone of high collision-induced correlations is now related to a broad domain, which can however still be isolated (see the part above the dashed line of fig. 12). A similar behaviour is found for 39.6 A.MeV Ta+Au and 80 A.MeV Au+Au INDRA data.

8. Selecting pseudo-equilibrated events with INDRA data

By selecting the events corresponding to the part below the dashed line of fig. 12, we select a sub-sample which corresponds to small collision-induced correlations. This sub-sample is potentially closer to full equilibration than the original sample. We will now look at the signal of negative heat capacity in the selected sub-sample of INDRA data.

The results for partial fluctuation measurements are presented in fig. 13 for 80 A.MeV Au+Au. We see that the effect of selecting small collision-induced correlations is to increase the fluctuations. Partial energy fluctuations reach large values which overcome the canonical expectation and lead to a negative heat capacity. The same conclusion is obtained with 39.6 A.MeV Ta+Au and 40 A.MeV Au+Au sytems.

The first goal here is not to be quantitative but rather to show that :

- the effect of collision-induced correlations is to reduce the fluctuations respect to a complete phase space filling,
- it seems possible within the collision sample to properly select a subset of events which presents the characteristics of an equilibrated projectile-like.

The first point is easy to understand : since collision-induced correlations lead to preferential directions, they hinder a complete randomization of phase space, and reduce the fluctuations. This fluctuation reduction can be either due to the fact that some of the detected fragments do not belong to the projectile-like source, or to the fact that the deexcitation of the projectile-like source is largely influenced by collision-induced correlations. In

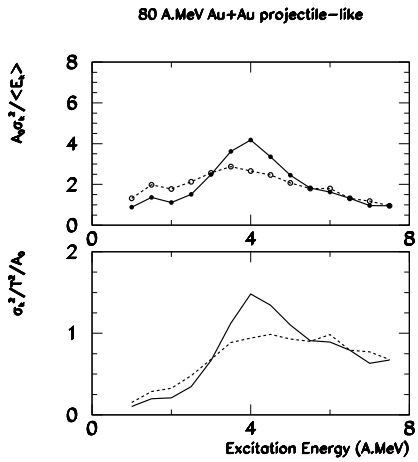

Figure 13: *Au+Au 80 A.MeV : projectile-like partial energy fluctuations versus excitation energy. Top : partial energy fluctuation (σ_k) normalized to the mean partial energy ($< E_k >$), bottom : σ_k normalized to the projectile-like temperature. The Partial energy fluctuations have been scaled with the size of the projectile-like source ($A_0 \pm 10\%$). Dashed lines are for the whole hypothetical projectile-like set. Full lines are for the small collision-induced correlations set.*

both cases the assumption that the calorimetrical energy represents a fully thermal excitation energy is wrong. Within both hypotheses, a part of the entrance channel energy is not relaxed. Studies of other signals, like bimodality, could give an answer to disentangle this situation.

The second point has to be confirmed with other systems, in particular asymmetric systems.

9. As a conclusion : INDRA versus MULTICS-Miniball

Now we come back to the MULTICS-Miniball INDRA comparison. We have seen that large collision-induced correlations are revealed by large p_{rel}. Removing those events has the effect to increase partial energy fluctuations. In fig. 14 is presented the c.m p_{rel} versus the angle of the biggest fragment detected in the forward c.m hemisphere (i.e. the hypothetical projectile-like). The diagram is plotted for 40 A.MeV Au+Au and the angle is the laboratory frame angle. This figure indicates that most of large collision-induced

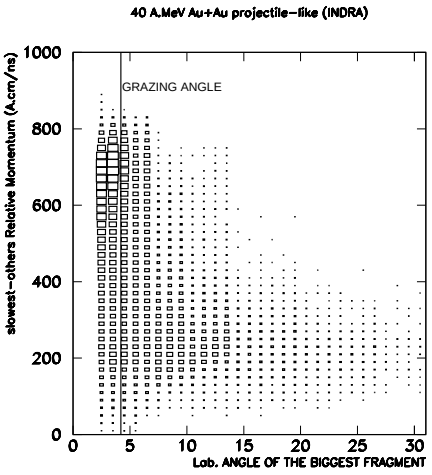

Figure 14: *40 A.MeV Au+Au : p_{rel} versus the laboratory frame angle of the biggest fragment detected in the forward c.m hemisphere. The line represents the system grazing angle.*

correlation events correspond to events where the biggest fragment flies at an angle below or about the grazing angle. In other words, dynamical processes are linked to biggest fragment characteristics close to the projectile ones.

The MULTICS-Miniball apparatus does not cover those small angles [6] and therefore the MULTICS-Miniball data are less sensitive to collision-induced correlations. Once the MULTICS-Miniball sample is compared to a subsample of INDRA data minimizing these dynamical correlations, the fragment partitions of the two data sets agree and in both cases corresponds to abnormal fluctuations. In other words, the MULTICS-Miniball detector acts as a small collision-induced correlation selector. The data are well reproduced by a statistical model [14], and are compatible with thermal equilibrium, in the sense that they seem to represent a random selection of deexcitation schemes from an excited Au nucleus.

An experiment [15] has been performed with the high granularity 4π CHIMERA detector [16] at LNS (Catania, Italy) to quantify this result.

To conclude, we would like to stress that : (i) for a proper statistical analysis one has to remove the collision-induced correlation events, (ii) for a proper dynamical analysis one has to remove the pseudo-equilibrated events. Both studies are complementary to measure fundamental properties of nuclei and nuclear matter.

Experiments performed with INDRA 4π detector at GANIL (France) and GSI (Germany).

References

[1] G. Bizard et al., Phys. Lett. **B302** (1993) 162.

[2] Ch. O. Bacri et al., Phys. Lett. **B353** (1995) 27.

[3] A.J. Cole, "Statistical Models for Nuclear Decay", IOP Publishing, (2000).

[4] Ph. Chomaz et al., **this conference**.

[5] F. Gulminelli et al., Phys. Rev. **E68** (2003) 026120.

[6] M. D'Agostino et al., Phys. Lett. **B473** (2000) 219.

[7] R. Bougault et al., XXXVIII International Winter Meeting on Nuclear Physics (2000), Bormio (Italy).

[8] O. Lopez, Nucl. Phys. **A685** (2001) 256c.

[9] B. Borderie et al., Phys. Rev. Lett. **86** (2001) 3252.

[10] M. F. Rivet et al., **this conference**.

[11] B. Tamain et al., **this conference**.

[12] J. Colin et al., Phys. Rev. **C67** (2003) 064603.

[13] M. D'Agostino et al., Nucl. Phys. **A699** (2002) 799.

[14] M. D'Agostino et al., Nucl. Phys. **A650** (1999) 329.

[15] R. Bougault et al. (REVERSE collaboration), 35 A.MeV Sn+Sn experiment.

[16] M. Alderighi et al., IEEE Trans. Nucl. Science **49** (2002) 334 and references therein.